

## THE $M/L_*$ RATIO OF YOUNG STAR CLUSTERS IN GALACTIC MERGERS

C. M. BOILY AND A. LANÇON

Observatoire Astronomique, 11 rue de l'Université, F-67000 Strasbourg, France; cmb@astro.u-strasbg.fr, lancon@astro.u-strasbg.fr

AND

S. DEITERS AND D. C. HEGGIE

School of Mathematics, University of Edinburgh, King's Building, Edinburgh EH9 3JZ, Scotland, UK; s.deiters@ed.ac.uk, d.c.heggie@ed.ac.uk

Received 2004 October 14; accepted 2004 December 23; published 2005 January 18

### ABSTRACT

We point out a strong time evolution of the mass-to-light conversion factor  $\eta$  commonly used to estimate masses of dense star clusters from observed cluster radii and stellar velocity dispersions. We use a gasdynamical model coupled with the Cambridge stellar evolution tracks to compute line-of-sight velocity dispersions and half-light radii weighted by the luminosity. Stars at birth are assumed to follow the Salpeter initial mass function in the range of  $0.15\text{--}17 M_\odot$ . We find that  $\eta$ , and hence the estimated cluster mass, increases by factors as large as 3 over timescales of 20 million years. Increasing the upper mass limit to  $50 M_\odot$  leads to a sharp rise of similar amplitude but in as little as 10 million years. Fitting truncated isothermal (Michie-King) models to the projected light profile leads to overestimates of the concentration parameter  $c$  of  $\delta c \approx 0.3$  compared to the same functional fit applied to the projected mass density.

*Subject headings:* galaxies: star clusters — methods: numerical — stars: luminosity function, mass function

*Online material:* color figure

### 1. INTRODUCTION

The formation of star clusters in bursts of star formation during galactic mergers has attracted much attention since the groundbreaking study by Schweizer (1986). Young clusters can account for  $\sim 20\%$  of the UV light flux of their sample starburst galaxies (compared with  $<1\%$  for the Milky Way; e.g., Meurer et al. 1995). Such numbers bring to focus the role that star formation in clusters plays in shaping the overall (galactic) stellar mass function. Prototypical cases in which cluster formation has been a spectacular manifestation of interaction-induced starbursts are the merging systems NGC 4038/39 (the Antennae) and the nearby galaxy M82 (recent interaction with M81). Many of the brightest clusters in these galaxies have estimated ages on the order of  $10^7$  yr, based on optical and near-IR spectra. High-resolution spectroscopic data and *Hubble Space Telescope* images have been used to measure velocity dispersions and estimate virial masses. The line-of-sight velocity dispersion  $\sigma_{1D}$  (LOSVD) relates to the mass  $M$  and projected half-light radius  $r_{ph}$  of a cluster in virial equilibrium through

$$M = \eta \frac{r_{ph} \sigma_{1D}^2}{G}, \quad (1)$$

where  $\eta$  is a dimensionless free parameter. A number of authors have set  $\eta \approx 10$  in their studies to derive  $M$  from equation (1) (Sternberg 1998; Mengel et al. 2002; Smith & Gallagher 2001; McCrady et al. 2003; Maraston et al. 2004). McCrady et al. (2003) give a derivation of this value of  $\eta$ . Mengel et al. (2002) quote a range from 5.6 to 9.7 for King (1966) models with a concentration parameter in the range of 0.5–2.5, which corresponds to most galactic globular clusters. We discuss the value of  $\eta$  in § 4. Dynamical masses derived from equation (1) have been compared to the stellar masses of synthetic populations, using both standard (field) and nonstandard stellar initial mass functions (IMFs; see Kroupa 2002 for a review). The data were found to be inconsistent with a universal IMF (Mengel et al. 2002; Smith & Gallagher 2001). In particular, several clusters

in M82 were found to be overluminous with respect to their estimated mass (low mass-to-light ratio,  $M/L_*$ ). This suggests that M82 clusters may form with a top-heavy stellar IMF (Smith & Gallagher 2001; McCrady et al. 2003).

These conclusions hinge on the precise value of  $\eta$ . The above studies have assumed no time variation of  $\eta$ , based on the belief that the structural parameters of young clusters are unlikely to have changed since the time they were born. A further implicit assumption made when applying equation (1) is that the stellar subpopulations sampled are all equally representative of the dynamics as a whole. This simplification is normally justified on the grounds that the estimated ages of the clusters are too short to allow for gradients in their spatial distribution and kinematics to develop from internal evolution. However, this train of thought stems from the derivation of a long relaxation time  $t_{th}$  for single-population clusters. Expressed in terms of the dynamical time  $t_{cr}$  evaluated at the half-mass radius  $R_h$  (Meylan & Heggie 1997, § 7):

$$\frac{t_{th}}{t_{cr}} \approx 0.138 \left(\frac{R_h}{R_g}\right)^{3/2} \frac{N}{\ln 0.4N}, \quad (2)$$

where  $R_g = GM^2/|W|$  is the gravitational radius and the ratio  $R_h/R_g \approx 1$  for a wide number of model fits to observed clusters. With a spectrum of masses, the trend toward equipartition of kinetic energy speeds up evolution, and mass segregation now develops on a timescale given by (Farouki & Salpeter 1982; Spitzer 1987)

$$\frac{t_{ms}}{t_{rh}} \approx \frac{\pi}{3} \frac{\langle m \rangle}{\max(m)} \frac{\bar{\rho}}{\rho} \left(\frac{R_h}{R_g}\right)^{3/2}, \quad (3)$$

where  $\bar{\rho} \equiv M/(4\pi R_h^3/3)$  is the mean density inside the half-mass radius (an overline denotes averaging over space, and angle brackets averaging by mass). The numerical coefficients entering equation (3) are derived from a stellar IMF and mass distribution. The Galactic-field IMF covers a range from  $\approx 0.08$

to  $\geq 60 M_{\odot}$  (O stars) and possibly all the way to  $\approx 100 M_{\odot}$  (Kroupa 2002). The mean mass for this IMF is  $\langle m \rangle \approx 1.33 M_{\odot}$  and gives a ratio  $\max(m)/\langle m \rangle \approx 100$ . This dramatically reduces the mass-segregation timescale (eq. [3]) and bears on the parameter  $\eta$  (through a time variation of  $r_{\text{ph}}$  and  $\sigma_{\text{1D}}$ ) since the brightest, most massive member stars are also those that undergo the most significant segregation and inward migration. The purpose of this Letter is to show with numerical modeling that, through this process, the mass-to-light conversion factor  $\eta$  of massive clusters evolves by a factor of a few over periods as short as 20 millions years, contrary to expectations of zero evolution.

## 2. NUMERICAL METHOD: GasTel

The equations of motion were integrated numerically based on the gasdynamical approach pioneered by Larson (1970) and developed further by Louis & Spurzem (1991) to include anisotropic velocity fields. The method leans on an analogy between the exchange of kinetic energy through star-star interactions and the classical heat-diffusion process of fluid dynamics (Lynden-Bell & Eggleton 1980; Heggie & Ramamani 1989). The implementation in spherical coordinates that we used is largely due to Louis & Spurzem (1991) and Giersz & Spurzem (1994) but is extended to include a spectrum of stellar masses (Spurzem & Takahashi 1995).

The mass spectrum is sampled at constant logarithmic increments in the interval  $[m_0, m_1]$ ; we used 14 bins in our standard runs ( $\delta \ln m \approx 0.329$ ). Star-star interactions (including those between stars of the same mass bin) lead to the diffusion of kinetic energy. Roughly speaking, the resulting change in the velocity dispersion of each mass bin causes a readjustment of the density profile. This is obtained using a semi-implicit Henyey integration. The gravitational potential is then updated by applying Poisson's equation (see Louis & Spurzem 1991).

We checked that the mass-segregation time (eq. [3]) obtained for GasTel is in quantitative agreement with  $N$ -body and Fokker-Planck integrators by computing the evolution of Plummer models with three species of stars (see Spitzer & Shull 1975, Fig. 1). Spurzem & Takahashi (1995) report excellent agreement with equation (3) from their two-component test calculations.

### 2.1. Stellar Evolution

The different mass components are evolved according to the Cambridge tracks (Pols et al. 1998; Hurley et al. 2000). The tracks are efficiently coded in the form of fitting functions of the kind first presented by Eggleton et al. (1989). The functions return the current bolometric luminosity, radius, mass, and metal abundance for a given time and initial metal abundance  $z_0$ ; in this contribution we set  $z_0 = 0.02$  (solar abundance) throughout.

A filter can be applied to the bolometric luminosity from model stellar atmospheres, and the total flux in a specified wave band read from the Basel stellar library (Lejeune et al. 1998). We have mapped the stellar luminosity near the strongest near-IR CO band head ( $\lambda \approx 2.2\text{--}2.29 \mu\text{m}$ ) and the Ca II triplet ( $\lambda \approx 8200\text{--}8600 \text{ \AA}$ ).

## 3. FLUX-WEIGHTED SCHEME AND STELLAR IMF

Low gradients in metal abundances in young clusters can be interpreted to imply a spatial distribution of stars independent

of their mass at the time the clusters formed (e.g., Suntzeff 1993). All the calculations presented here have no built-in segregation initially.

The flux-weighted LOSVD is obtained first by averaging the square velocity dispersion within a projected radius  $R$  for a given stellar mass and then by averaging over all stellar masses, using as statistical weight the total luminosity  $\Lambda_{\lambda}^{\delta\lambda}(m)$  of mass component  $m$  over a wavelength interval  $\delta\lambda$  centered on  $\lambda$ . The mean square velocity of stars of mass  $m$ ,  $\bar{\sigma}_m^2$ , is computed from their surface density  $\Sigma_m$ :

$$\bar{\sigma}_m^2(R) = \int_0^R \sigma_m^2(r) \Sigma_m(r) \pi dr^2 \Big/ \int_0^R \Sigma_m(r) \pi dr^2.$$

The dispersions  $\bar{\sigma}_m^2$  are summed over all masses using the luminosity as statistical weight,

$$\langle \sigma_{\lambda}^2 \rangle = \int_{m_0}^{m_1} \bar{\sigma}_m^2 \Lambda_{\lambda}^{\delta\lambda}(m[t]) n(m) d \ln m / \mathcal{W}_{\lambda}, \quad (4)$$

where  $n(m)$  is the number of stars in the logarithmic mass interval  $\ln m, \ln m + \delta \ln m$ . The normalization constant  $\mathcal{W}_{\lambda}$  is the total light flux at wavelength  $\lambda$  from all stars at time  $t$ . Note that  $n(m)$  in equation (4) refers to the IMF. All time dependencies are encapsulated in  $\Lambda_{\lambda}^{\delta\lambda}(m[t])$  and  $\bar{\sigma}_m^2$ .

For the mass range  $1\text{--}60 M_{\odot}$  (up to O stars), the single-star IMF is well represented by a Salpeter (1955) power law,  $n(m) d \ln m \propto m^{-2.35} dm$ . We set the mass range  $[m_0, m_1]$  to cover two decades, from  $0.15$  to  $17 M_{\odot}$  (spectral types M5–B5). Note that solar neighborhood data favor an IMF that flattens out below  $1 M_{\odot}$  (Scalo 1986; Kroupa et al. 1993), so our choice of a Salpeter IMF may seem artificial. However, for the chosen mass range, we compute  $\langle m \rangle / m_1 \approx 0.025$ , a ratio nearly identical to that obtained from the Galactic-field IMF. Thus, our choice of mass function and mass range yields a conservative mass-segregation timescale compared with other IMFs when the latter are extended beyond  $60 M_{\odot}$ .

## 4. RESULTS

The runtime of our calculations was set to 50 Myr. All models were scaled to  $N = 500,000$  member stars and a total mass of  $M \approx 2 \times 10^5 M_{\odot}$ . We vary the dynamical evolution time between runs by constructing models with different sizes and central densities, while keeping the total mass, and  $N$ , constant. Mengel et al. (2002) fitted the light profile of young Antennae clusters with King models of dimensionless parameter  $\Psi/\sigma^2 = 6\text{--}9$ . We first set up three models with identical  $\Psi/\sigma^2 = 6$  King parameters, each with a different half-light radius (Table 1). The model labeled ‘‘M82-F’’ has a mean surface density  $\approx 1.5 \times 10^4 M_{\odot} \text{ pc}^{-2}$ , or half the value we derive for that cluster from the data of Smith & Gallagher (2001). The densest model is labeled ‘‘R136,’’ in reference to the 30 Doradus cluster (with a central volume density of  $\sim 10^6 M_{\odot} \text{ pc}^{-3}$ ; Brandl et al. 1996). Finally, a third low-density model was evolved for comparison (labeled ‘‘Low’’).

We start with the densest model, R136, for which we compute the shortest relaxation time  $t_{\text{rh}}$ . Since  $M$ ,  $r_{\text{ph}}$ , and  $\langle \sigma_{\lambda}^2 \rangle$  are all known from the simulations, we solve for  $\eta$  directly from equation (1). The run of  $\eta$  in time is displayed in Figure 1a. Three curves are shown, corresponding to bolometric light and filters centered on the CO continuum and the Ca II triplet. The

TABLE 1  
 PARAMETERS OF THE MODELS

Model	$\Psi/\sigma^2$	$t_{\text{ms}}$ (Myr)	$r_{\text{ph},0}$ (pc)	$\hat{r}_{\text{ph}}$ (pc)	$\Sigma_0(0)$ ( $10^5 M_{\odot} \text{pc}^{-2}$ )	$\bar{\Sigma}_0(r_{\text{ph}})$ ( $10^5 M_{\odot} \text{pc}^{-2}$ )	$\eta_0$	$\hat{\eta}$	$\delta c$
R136 .....	6	9.3	1.01	$0.51 \pm 0.03$	0.885	0.417	8.15	$18.5 \pm 1$	0.29
M82-F .....	6	15.9	1.46	$1.02 \pm 0.06$	0.474	0.224	8.15	$12.6 \pm 0.7$	...
Low .....	6	47.9	3.05	$2.84 \pm 0.05$	0.109	0.051	8.15	$8.54 \pm 0.06$	...
Plummer .....	4.5	7.5	1.05	$0.62 \pm 0.03$	0.606	0.410	8.20	$16 \pm 1$	0.23
	9	25.7	0.95	$0.49 \pm 0.02$	5.232	0.440	7.76	$19 \pm 4$	0.29

NOTES.—All models have a total mass  $M = 2 \times 10^5 M_{\odot}$ . We set  $R_h = R_g/2$  and  $\rho = \bar{\rho}$  in eq. (3) to average  $t_{\text{ms}}$ . The subscript 0 denotes  $t = 0$ ; hats denote time averages over the last 25 Myr of evolution. The last column gives the increase of the concentration parameter  $\delta c$  for a few cases (§ 5).

rapid increase of  $\eta$  from an initial value of  $\approx 8.2$  is striking. After 15 Myr of evolution,  $\eta$  has more than doubled. The projected half-light radius  $r_{\text{ph}}$  is displayed alongside  $\eta$ . In all the cases,  $r_{\text{ph}}$  decreases steadily in time, a direct result of the migration of massive stars toward the center. The general trend and quantities are not sensitive to the wave band adopted, for both  $\eta$  and  $r_{\text{ph}}$ . Note the slow but systematic rise of  $\eta$  after  $\approx 35$  Myr, when  $\eta > 20$  (a factor of  $> 2.5$  from its initial value; Fig. 1a).

The LOSVD changes relatively little over time in comparison: we measure a monotonic decrease of  $\langle \sigma_{\lambda} \rangle$  from  $\approx 10.4$  to  $9.3 \text{ km s}^{-1}$  (or  $-10.6\%$ ) for the system as a whole, although for individual components, evolution was more significant, down  $\approx 30\%$  for the most massive stars, while the lightest component enjoys an increase of a comparable magnitude. These effects can all be traced back to the dynamical mass segregation.

The time evolution of  $\eta$  for all three models is displayed in Figure 1b; we have plotted only the results for the bolometric light for clarity. Both  $\eta$  and  $r_{\text{ph}}$  for the “Low” model stay essentially constant throughout. However, M82-F (with an initial surface density  $> 10^4 M_{\odot} \text{pc}^{-2}$ ) shows unmistakable evolution, suggesting that for clusters of such mean surface density

or higher, we may no longer presume a time-independent mass-to-light conversion factor  $\eta$ .

## 5. DISCUSSION AND FUTURE WORK

When the projected density of massive star clusters exceeds a few  $\times 10^4 M_{\odot} \text{pc}^{-2}$ , the mass-to-light conversion factor  $\eta$  used to derive the mass in equation (1) may increase by a factor as large as 3 over timescales of a few  $\times 10^7 \text{ yr}$  (cf. Fig. 1b and Table 1). Clusters with low surface density have long mass-segregation timescales and constant  $\eta$ . When we compare clusters with a similar mean surface density of  $\approx 4 \times 10^4 M_{\odot} \text{pc}^{-2}$  but with different central densities initially, the results indicate that the increase in  $\eta$  is an increasing function of the initial central density (Table 1). Thus, the drift of heavy stars toward the center can considerably bias mass estimates of clusters centrally peaked at birth. The resolved cluster R136 (NGC 2070) in the 30 Doradus complex is a case in point: its central volume density may be as high as  $\sim 10^6 M_{\odot} \text{pc}^{-3}$  with an estimated spherical half-mass radius of  $\sim 1 \text{ pc}$  (Brandl et al. 1996). Several clusters in the Antennae or M82 have estimated masses of  $\sim 10^6 M_{\odot}$  and projected half-light radii of approxi-

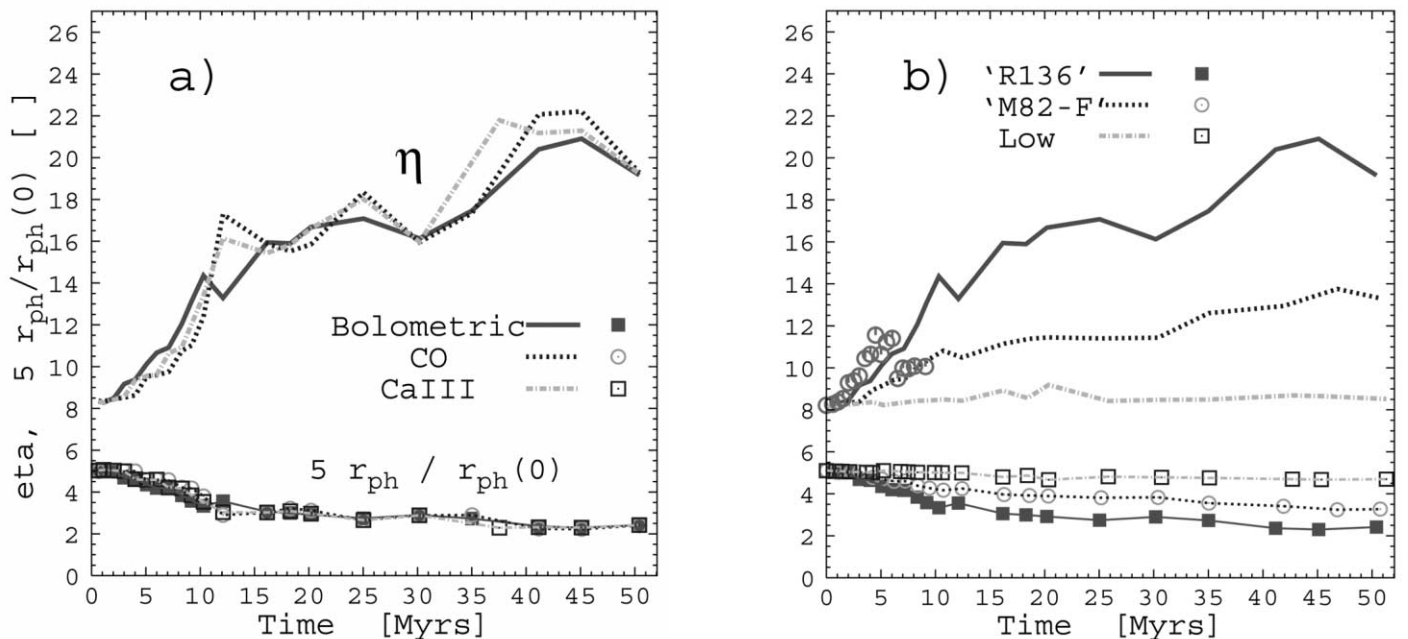


FIG. 1.—Parameter  $\eta$  and half-light radius  $r_{\text{ph}}$  vs. time. The initial models were unsegregated King  $\Psi/\sigma^2 = 6$  models. (a) Results using filters at three different wave bands (see text for details). (b) Results for models with different initial surface densities (see Table 1). When the mass range is increased from 17 to  $50 M_{\odot}$ ,  $\eta$  rises sharply over the first 10 Myr (open circles, model M82-F); thereafter it rejoins the curve displayed. [See the electronic edition of the Journal for a color version of this figure.]

mately a few parsecs. Smith & Gallagher (2001) derive  $M = 1.2 \times 10^6 M_{\odot}$  and  $r_{\text{ph}} \approx 2.8$  pc for the cluster M82-F. The mean surface density of this cluster is  $\sim 2.4 \times 10^4 M_{\odot} \text{pc}^{-2}$  inside  $r_{\text{ph}}$ , which is comparable to our model M82-F; for comparison, our model R136 had a mean density twice as high. All calculations were done for a membership of  $N = 500,000$ , a factor of 2 lower than rich starburst clusters. This may serve to accelerate evolution compared with actual massive clusters (cf. eq. [2]). We recall that our choice of an upper mass  $m_1 < 20 M_{\odot}$  yields a mass-segregation timescale that is a factor of 3 longer than if we had included O stars. A rerun of M82-F with a mass spectrum widened to  $50 M_{\odot}$  yielded a rapid increase of  $\eta$  over a shorter, 10 Myr timescale (*open circles*, Fig. 1*b*). Therefore, the evolution of  $\eta$  through the mass segregation of stars is a sensitive function of both the IMF and the cluster surface density profiles. We mention that the cluster M82-F has an age of  $\approx 60 \pm 20$  Myr, by which time the increase of  $\eta$  is maximum. This larger value of  $\eta$  would go some way toward solving the apparent overluminosity of young M82 clusters with respect to a standard IMF. Recent work on M82-F has highlighted the possibility of strong mass segregation in that cluster (McCraday et al. 2005).

The strong evolution of  $\eta$  for model R136 (Fig. 1*a*) suggested to us to compare functional fits to the total surface density and luminosity profiles. We performed least-squares fits (Press et al. 1992) using King profiles on the simulation grid out to  $5r_{\text{ph}}$ . Doing this for model R136 after 35 Myr of evolution, we

found a best fit to the radial luminosity profile (cf. § 3) that gave a King parameter  $\Psi/\sigma^2 \approx 7.6$  (compared with  $\approx 6$  for the run of density). The concentration parameter  $c = \log |r_i/r_0|$  increases by  $\approx 0.45$  as  $\Psi/\sigma^2$  runs from 6 to 7.6. Since the truncation radius  $r_t$  remains constant, the central region seemingly shrinks by a factor of  $\approx 2.8$  compared with the surface density. Table 1 gives values of  $\langle \eta \rangle$  and  $\langle r_{\text{ph}} \rangle$  averaged over the last 25 Myr of evolution for this and two other models, which also show increased concentration. The effect can be cast in the context of a whole population of clusters as detected in interacting galaxies such as the Antennae (NGC 4038/9) or M82. Our modeling indicates that the clusters should be even more massive than estimated until now, and less concentrated. Therefore, their binding energy per unit mass will be less than deduced from profiling the light. This would in turn reduce their lifetime within the host galaxy. However, it has not escaped our attention that fitting the light flux would require a convolution with the point-spread function of an instrument that would allow us to make direct comparisons with observations. More detailed models will be presented in a follow-up study (J.-J. Fleck et al. 2005, in preparation).

We thank the anonymous referee for a first-class report. C. M. B. and A. L. thank the ASSNA and the PNG (France) for financial support. D. C. H. and S. D. warmly thank the Observatoire de Strasbourg for their hospitality during the course of this research.

#### REFERENCES

- Brandl, B., et al. 1996, ApJ, 466, 254  
 Eggleton, P. P., Tout, C. A., & Fitchett, M. J. 1989, ApJ, 347, 998  
 Farouki, R. T., & Salpeter, E. E. 1982, ApJ, 253, 512  
 Giersz, M., & Spurzem, R. 1994, MNRAS, 269, 241  
 Heggie, D. C., & Ramamani, N. 1989, MNRAS, 237, 757  
 Hurley, J. R., Pols, O. R., & Tout, C. A. 2000, MNRAS, 315, 543  
 King, I. R. 1966, AJ, 71, 64  
 Kroupa, P. 2002, Science, 295, 82  
 Kroupa, P., Tout, C. A., & Gilmore, G. 1993, MNRAS, 262, 545  
 Larson, R. B. 1970, MNRAS, 147, 323  
 Lejeune, T., Cuisinier, F., & Buser, R. 1998, A&AS, 130, 65  
 Louis, P. D., & Spurzem, R. 1991, MNRAS, 251, 408  
 Lynden-Bell, D., & Eggleton, P. P. 1980, MNRAS, 191, 483  
 Maraston, C., Bastian, N., Saglia, R. P., Kissler-Patig, M., Schweizer, F., & Goudfrooij, P. 2004, A&A, 416, 467  
 McCraday, N., Gilbert, A. M., & Graham, J. R. 2003, ApJ, 596, 240  
 McCraday, N., Graham, J. R., & Vacca, W. D. 2005, ApJ, in press (astro-ph/0411256)  
 Mengel, S., Lehnert, M. D., Thatte, N., & Genzel, R. 2002, A&A, 383, 137  
 Meurer, G. R., Heckman, T. M., Leitherer, C., Kinney, A., Robert, C., & Garnett, D. R. 1995, AJ, 110, 2665  
 Meylan, G., & Heggie, D. C. 1997, A&A Rev., 8, 1  
 Pols, O. R., Schroder, K.-P., Hurley, J. R., Tout, C. A., & Eggleton, P. P. 1998, MNRAS, 298, 525  
 Press, W. H., Teukolsky, S. A., Vetterling, W. T., & Flannery, B. P. 1992, Numerical Recipes in FORTRAN (2nd ed.; Cambridge: Cambridge Univ. Press)  
 Salpeter, E. E. 1955, ApJ, 121, 161  
 Scalo, J. M. 1986, Fundam. Cosmic Phys., 11, 1  
 Schweizer, F. 1986, Science, 231, 227  
 Smith, L. J., & Gallagher, J. S., III. 2001, MNRAS, 326, 1027  
 Spitzer, L., Jr. 1987, Dynamical Evolution of Globular Clusters (Princeton: Princeton Univ. Press)  
 Spitzer, L., Jr., & Shull, J. M. 1975, ApJ, 201, 773  
 Spurzem, R., & Takahashi, K. 1995, MNRAS, 272, 772  
 Sternberg, A. 1998, ApJ, 506, 721  
 Suntzeff, N. 1993, in ASP Conf. Ser. 48, The Globular Clusters–Galaxy Connection, ed. G. H. Smith & J. P. Brodie (San Francisco: ASP), 167